Pure Appl. Geophys. 175 (2018), 633–645

https://doi.org/10.1007/s00024-017-1716-6

Pure and Applied Geophysics

A Dimensional Analysis Method for Improved Load–Unload Response Ratio

Yue Liu[1] and Xiang-chu Yin[1,2]

Abstract—The load–unload response ratio (LURR) method is proposed to measure the damage extent of source media and the criticality of earthquake. Before the occurrence of a large earthquake, anomalous increase in the time series of LURR within the certain temporal and spatial windows has often been observed. In this paper, a dimensional analysis technique is devised to evaluate quantitatively the magnitude and time of the ensuing large earthquake within the anomalous areas derived from the LURR method. Based on the π-theorem, two dimensionless quantities associated with the earthquake time and magnitude are derived from five parameters (i.e. the seismic energy (E_S), the average seismic energy (E_W), the maximum value of LURR's seismogenic integral (I_{PP}), the thickness of seismogenic zone (h), the time interval from I_{PP} to earthquake (T_2), and the shear strain rate ($\dot{\gamma}$)). The statistical relationships between the earthquakes and the two dimensionless quantities are derived by testing the seismic data of the 50 events of $M4.5 \sim 8.1$ occurred in China since 1976. In earthquake prediction, the LURR method is used to detect the areas with anomalous high LURR values, and then our dimensional analysis technique is applied to assess the optimal critical region, magnitude, and time of the ensuing event, when its seismogenic integral is peaked (I_{PP}). As study examples, we applied this approach to study four large events, namely the 2012 $M_S5.3$ Hami, 2015 $M_S5.8$ Alashan, 2015 $M_S8.1$ Nepal earthquakes, and the 2013 Songyuan earthquake swam. Results show that the predicted location, time, and magnitude correlate well with the actual events. This provides evidence that the dimensional analysis technique may be a useful tool to augment current predictive power of the traditional LURR approach.

Key words: Load–unload response ratio, dimensional analysis, π-theorem, prospectively, seismic hazard evaluation.

[1] Institute of Earthquake Forecasting, China Earthquake Administration, No. 63, Fuxing Road, Haidian District, Beijing 100036, China. E-mail: liuyue@cea-ies.ac.cn; xcyin2012@163.com

[2] State Key Laboratory of Nonlinear Mechanics, Institute of Mechanics, Chinese Academy of Sciences, Beijing 100019, China.

1. Introduction

The physical essence of an earthquake lies in the nonlinear far-from-equilibrium damage process along with the random distribution of initial defects within the source media, causing the complexity in the prediction of earthquakes. To understand earthquake occurrence, physics-based modeling of the entire seismogenic process is essentially important (Yu and Zhu 2010). From the viewpoint of mechanics, occurrence of an earthquake is the damage, instability or failure of the focal media and accompanied with a rapid release of energy (Bowman et al. 1998; Kasahara 1981; Scholz et al. 1972). The load-unload response ratio (LURR) theory (Yin 1987, 1993; Yin et al. 1995) is proposed to depict the tempo-spatial variation of damage of source media in this regard (Bai et al. 2002; Kachanov 1986; Lemaitre 1992; Li et al. 2000; Yin et al. 2006). This method is based on measuring the ratio between Benioff strains released during the time periods of loading and unloading, corresponding to the Coulomb Failure Stress change induced by Earth tides on optimally oriented faults (Melchior 1983). The value of LURR is defined as

$$Y = \frac{\sum_{i=1}^{N+} E_i^m}{\sum_{j=1}^{N-} E_i^m}, \tag{1}$$

where, N_+ and N_- represent the numbers of events that occurred during the loading and unloading stages. When $m = 1/2$, E^m denotes the Benioff strain. Analysis of the anomalies in the LURR time series provides us with seismic potential evaluation with estimates of all the crucial parameters provided such as earthquake location, time, and magnitude. In the retrospective studies, hundreds of earthquake forecasting examples have been performed, most of which were preceded with anomalous high LURR values (Liu et al. 2012; Song et al. 2000; Wang et al. 2004; Yin et al. 2006, 2008, 2012, 2013; Yu et al. 2011, 2016; Zhang 2006; Zhang and Zhuang 2011; Zhang et al. 2013). In the prospective studies (Yu et al. 2013, 2015, 2016), the seismic hazard region is usually determined by evaluating its LURR evolution in recent years. In conventional practice, we usually set an anomaly threshold for LURR. But the lack of quantitative assessment for the confidence level of the LURR peaks may sometimes compromise the reliability of the forecast.

Previous studies have illustrated that the forecasting time scale (T_2), from the peak LURR to the earthquake, is a statistical function of the magnitude of detection earthquakes (Zhang 2006):

$$T_2 = 60 \times (1 - 2.3 \times 10^{-0.08M}). \tag{2}$$

According to the above equation to make prediction, for example the Xinjiang region, China, however, does show some noticeable differences between the prediction results and the facts. Other impacts such as the movement of the fault, regional tectonic stress–strain setting should also be taken into account.

In this paper, we experiment a revised approach to assess the forecasting effectiveness of the LURR anomalies by combining the LURR method with the dimensional analysis technique, in which the historical seismic activity and shear strain rate during seismogenic process are taken into account (Liu et al. 2012; Liu 2014; Yin et al. 2012, 2013). To show the validity of the approach, four earthquakes are chosen as the examples, namely the 2012 M_S5.3 Hami earthquake, the 2013 Songyuan earthquake swarm, 2015 M_S5.8 Alashan earthquake, and the 2015 M_S8.1 Gorkha, Nepal earthquake.

2. *Two Dimensionless Quantities and LURR Anomalies*

In order to augment the evaluation of the magnitude and time of a future event as well as the critical region, in addition to the parameters such as the seismic activities and the focal mechanism, the shear strain rate (representing the regional tectonic stress–strain setting) should also be taken into consideration (Aki 1965; Gutenberg and Richter 1944). Thus, there are six physical quantities for assessment of the confidence level of a LURR anomaly: the seismic energy of E_S, the seismic energy density of E_W, the maximum value of LURR seismogenic integral I_t (I_{PP}), the thickness of seismogenic zone (h), the time interval from I_{PP} to the earthquake (T_2), and the shear strain rate in situ ($\dot{\gamma}$). Here, I_t is defined as

$$I_t = \iint_{Y>1} Y \mathrm{d}x\mathrm{d}y = \overline{Y}A, \tag{3}$$

where Y is the value of LURR, $\overline{Y}$ is the average value of LURR for the area of A. Please note that if $Y > 1$, the region is retained and otherwise, discarded.

We use dimensional analysis technique to deal with these parameters. Dimensional analysis is an effective approach to revealing the physical laws governing nature phenomena (Sedov 1959; Tan 2011; Zohuri 2015) and the main procedures can be outlined as follows:

1. To classify the physical quantities of a given phenomenon;
2. to find the correlation that connects the physical quantities;
3. to find causality that connects the physical quantities.

In various branches of mechanics, applications of the dimensional analysis to natural phenomena and technical problems have yielded a large number of results (Buckingham 1914; Tan 2011; Zohuri 2015). In the viewpoint of mechanics, the energy accumulation during the earthquake preparation process is closely related to the elasticity of the crust media and the loading rate (Yang et al. 2008; Zubovich et al. 2010). According to this technique, the six physical quantities (E_S, E_W, I_{PP}, h,$\dot{\gamma}$, and T_2) correspond to three fundamental units (length: L, time: T and mass-M_m) which are used to establish dimensionless relationship. Detailed units of the six physical quantities are as follows:

E_S: with the unit of J and the dimension of $[E_S] = [M_m L^2]$.

E_W: with the unit of $J/(\mathrm{km}^2 \cdot a)$ and the dimension of $[E_W] = [M_m T^{-1}]$, depicting the average intensity of seismic activity in a region (Reches and Lockner 1994a; Jaume and Sykes 1999; Yin et al.

2002; Liu 2014). In this study, the catalog from 1900 to 2009 is used to calculate E_W. So the time interval T is 110 years. The radiation radius R of seismic energy is determined according to the scaling relationship between the critical region size of LURR and the earthquake magnitude (Yin et al. 2002, 2006), which is associated with energy accumulation and releasing:

$$\lg R = 0.087 + 0.34 M_S \tag{4}$$

For a point (x, y), E_W is calculated by the following formula (5):

$$E_W = \frac{k}{T}\sum_{i=1}^{n}\frac{w_i E_{Si}}{\pi R_i^2}, \tag{5}$$

$$w_i = \left(1 - \frac{r_i}{R_i}\right)^{\lambda}, \ (r_i \le R_i), \tag{6}$$

E_{Si} is the seismic energy of the ith earthquake. r_i is the distance between the study point (x, y) and the epicenter of the ith earthquake, n is the number of earthquakes satisfying the condition of $r_i \le R_i$. w is the weighted factor, and the index $\lambda = 1$ in this paper. In order to conform to $\int_0^{2\pi}\int_0^{R} kw\mathrm{d}r\mathrm{d}\theta = 1$, k is equal to 3.

I_{PP}: with the unit of km^2 and the dimension of $[I_{PP}] = [L^2]$.

h: the seismogenic depth, with the unit of km and the dimension of $[h] = [L]$.

T_2: with the dimension of $[T_2] = [T]$.

$\dot{\gamma}$: with the unit of 10^{-9}/a and the dimension of $[\dot{\gamma}] = [T^{-1}]$. The shear strain rate, reflecting the shear stress loading rate caused by tectonic stress, is proportional to the shear stress rate when the system is in the elasticity phase. The distribution of $\dot{\gamma}$ for Chinese mainland is obtained from the GPS measured results (Shen et al. 2003; Gu et al. 2001; Li et al. 2004; Jiang et al. 2003).

According to the π-theorem (Sedov 1959; Zohuri 2015), two independent dimensionless quantities could be derived from above 6 physical parameters. The LURR is proposed for measuring the degree of closeness to instability for a nonlinear system. The selection of the optimal critical region size of precursory LURR anomaly is closely related to the magnitude of the detection earthquake Yin et al. (2002). Thereby, we let

$$\pi_0 = h/\sqrt{I_{PP}}, \tag{7}$$

to depict the critical region size and the earthquake magnitude, i.e. $\pi_0 = f(M)$.

In fact, E_S is the dependent variable, while the E_W, I_{PP} and $\dot{\gamma}$ are independent variables. The dimensionless relationship is established as

$$[E_S] = [E_W]^{\alpha_1} \cdot [I_{PP}]^{\alpha_2} \cdot [\dot{\gamma}]^{\alpha_3}. \tag{8}$$

Corresponding dimension form can be written as:

$$[M_m \cdot L^2] = [M_m \cdot T^{-1}]^{\alpha_1} \cdot [L^2]^{\alpha_2} \cdot [T^{-1}]^{\alpha_3}. \tag{9}$$

In the left side of Eq. (9), the index of M_m, L, and T are 1, 2, and 0, respectively. In the right side, the index of M_m, L, and T are α_1, $2\alpha_1$, and $-\alpha_1 - \alpha_3$. So we can get

$$\begin{cases} 1 = \alpha_1 \\ 2 = 2\alpha_2 \\ 0 = -\alpha_1 - \alpha_3; \end{cases} \tag{10}$$

then

$$\alpha_1 = 1, \alpha_2 = 1, \alpha_3 = -1. \tag{11}$$

Combining Eqs. (8) and (11), we can get

$$[E_S] = [E_W]^1 \cdot [I_{PP}]^1 \cdot [\dot{\gamma}]^{-1}. \tag{12}$$

From the right side of the above formula, we have

$$E_d = \frac{E_W \cdot I_{pp}}{\dot{\gamma}}, \tag{13}$$

where E_d is associated with the accumulated energy during the establishment of the criticality, with the unit of J. From Eqs. (12) and (13), one dimensionless quantity (π_1) can be defined as

$$\pi_1 = \frac{E_S}{E_d}. \tag{14}$$

Similar to π_0, π_1 is also determined by magnitude of the detection earthquake, so $\pi_1 = f(\pi_0) = g(M)$.

On the other hand, the occurrence time of earthquake should also be taken into account. The quantity of $T_2 \cdot \dot{\gamma}$ is the loading value from I_{PP} to earthquake, and it is related to earthquake time and magnitude. So another dimensionless quantity is defined as

$$\pi_2 = \pi_1 \cdot (T_2 \cdot \dot{\gamma}). \quad (15)$$

To establish the relationship between π_1,π_2 and the magnitude of detection earthquakes, we apply the dimensionless analysis technique to 50 earthquakes with magnitude of $4.5 \leq M_S \leq 8.1$ that occurred in Chinese mainland since 1976. The location of the earthquakes is shown in Fig. 1.

The log-linear relationship between the magnitude and the two dimensionless quantities is shown in Figs. 2 and 3.

Results indicate a roughly linear increase of π_1 and π_2 along with M, shown as (Liu et al. 2012; Yin et al. 2012, 2013):

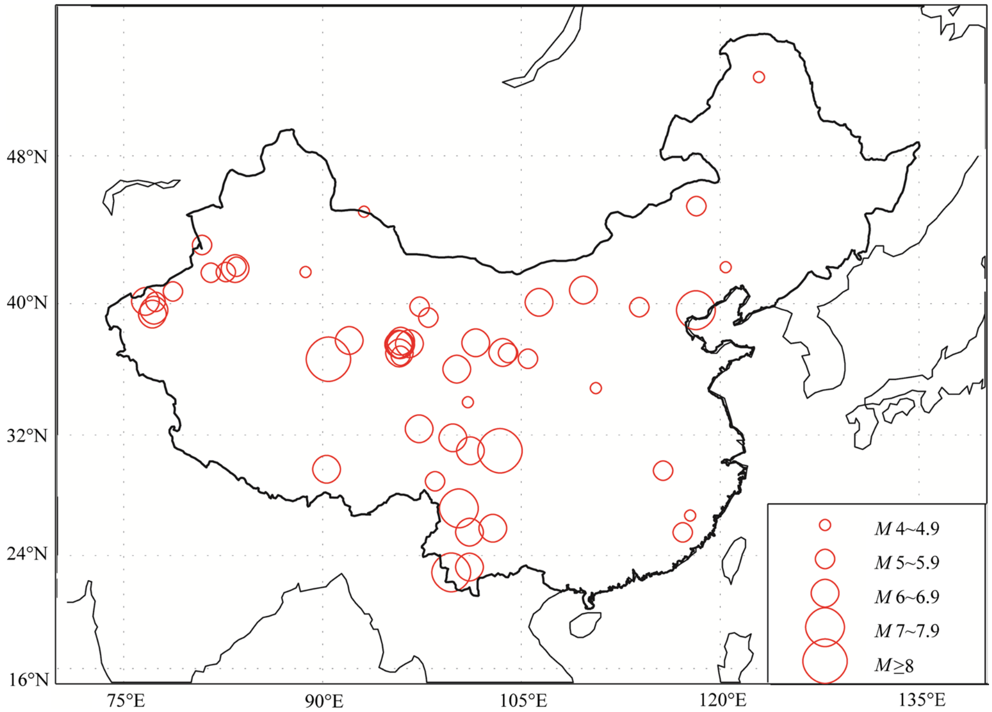

Figure 1

Locations of earthquakes selected for the dimensional analysis: the 50 M4.5 $\sim$ 8.1 earthquakes occurred in Chinese mainland since 1976. 1976-03-20 *M*4.7 Tuokesun, Xinjiang Autonomous Region, 1976-07-28 *M*7.8 Tangshan, Hebei province, 1976-09-23 *M*6.2 Bayinmuren, Inner Mongolia Autonomous Region, 1977-01-19 *M*6.3 Geermu, Qinghai province, 1977-07-23 *M*5.4 Kuche, Xinjiang Autonomous Region, 1979-03-15 *M*6.8 Puer, Yunnan province, 1979-03-29 *M*6.0 Kuche, Xinjiang Autonomous Region, 1979-03-29 *M*6.2 Yushu, Qinghai province, 1981-01-24 *M*6.9 Daofu, Sichuan province, 1982-04-14 *M*5.5 Haiyuan, Ningxia province, 1982-06-16 *M*6.0 Ganzi, Sichuan province, 1985-08-12 *M*5.3 Geermu, Qinghai province, 1985-04-18 *M*6.2 Luquan, Yunnan province, 1986-08-26 *M*6.5 Menyuan, Qinghai province, 1988-11-6 *M*7.4 Lancang, Yunnan province, 1990-01-14 *M*6.5 Mangya, Qinghai province, 1990-04-26 *M*6.9 Gonghe, Qinghai province, 1990-10-20 *M*6.1 Tianzhu, Gansu province, 1995-09-26 *M*5.2 Baicheng, Xinjiang Autonomous Region, 1996-02-3 *M*7.0 Lijiang, Yunnan province, 1996-03-19 *M*6.9 Atushi, Xinjiang Autonomous Region, 1996-05-03 *M*6.4 Baotou, the Inner Mongolia Autonomous Region, 1996-07-17 *M*4.6 Inner Mongolia Autonomous Region, 1997-01-21 *M*6.4 Jiashi, Xinjiang Autonomous Region, 1997-05-31 *M*5.2 Yongan, Fujian province, 1998-07-11 *M*4.5 Shanxi province, 1999-03-15 *M*5.6 Baicheng, Xinjiang Autonomous Region, 1999-06-01 *M*5.0 Mangkang, Tibet Autonomous Region, 2000-06-06 *M*5.9 Jingtai, Gansu province, 1999-11-01 *M*5.6 Yanggao, Shanxi province, 2001-11-04 *M*8.1 West of Kunlun mountain, 2002-12-14 *M*5.9 Yumen, Gansu province, 2003-02-24 *M*6.8 Kashi, Xinjiang Autonomous Region, 2003-04-17 *M*6.6 Delingha, Qinghai province, 2004-03-04 *M*4.8 Maqu, Gansu province, 2004-03-24 *M*5.9 Inner Mongolia Autonomous Region, 2005-01-24 *M*4.7 Heilongjiang province, 2005-11-26 *M*5.7 Jiujiang-Ruichang, Jiangxi province, 2007-03-13 *M*4.7 Shunchang, Fujian province, 2008-01-17 *M*4.7 Yili, Xinjiang Autonomous Region, 2008-05-12 *M*4.7 Wenchuan, Sichuan province, 2008-08-06 *M*4.9 Aletai, Xinjiang Autonomous Region, 2008-10-06 *M*6.6 Lasa, Tibet Autonomous Region, 2008-11-10 *M*6.3 Haixi, Qinghai province, 2009-01-25 *M*5.0 Chabuchaerxi, Xinjiang Autonomous Region, 2009-02-20 *M*5.2 Keping, Xinjiang Autonomous Region, 2009-04-19 *M*5.5 Aheqi, Xinjiang Autonomous Region, 2009-04-22 *M*5.0 Atushi, Xinjiang Autonomous Region, 2009-07-09 *M*6.0 Chuxiong, Yunnan province, 2009-08-28 *M*6.4 Haixi, Qinghai province

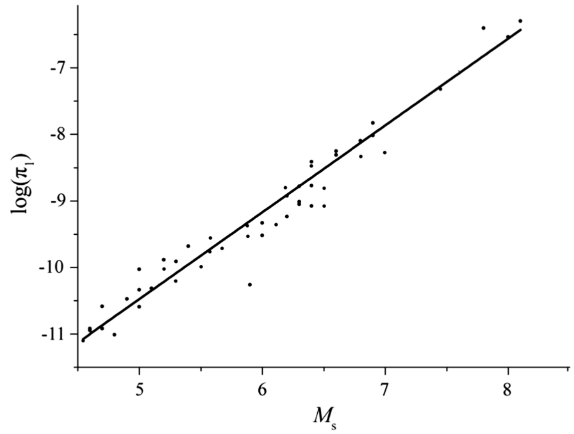

Figure 2
The log-linear relationship between M_S and π_1

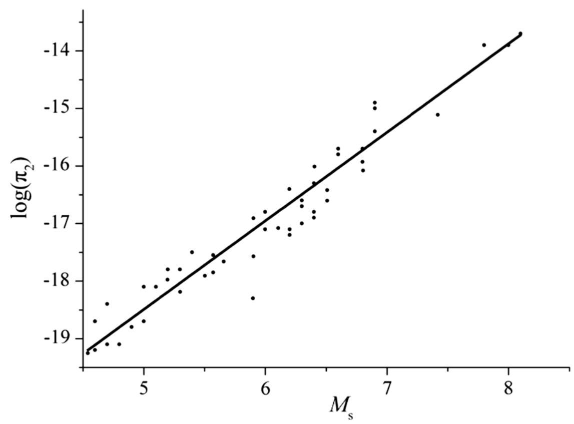

Figure 3
The log-linear relationship between M_S and π_2

$$\log \pi_1 = 1.31 M_S - 17, \tag{16}$$

and

$$\log \pi_2 = 1.53 M_S - 26.14. \tag{17}$$

For the linear relation of $\log\pi_1$ and M_S, the standard error for intercept and slope is 0.29 and 0.05, respectively, and the Adj. R^2 is 0.96. For $\log\pi_2$ and M_S, the standard error for intercept and slope is 0.43 and 0.07, respectively, and the Adj. R^2 is 0.94.

Combining formulas (14) and (15) with formulas (16) and (17), the derived magnitude (M_{Sd}) and T_{2d} are expressed as follows (Liu et al. 2012; Yin et al. 2012, 2013):

$$M_{Sd} = 5.14 \lg E_d - 112.08, \tag{18}$$

$$T_{2d} = \frac{8.5 \times 10^{-30.8} \times E_d \times 10^{0.03 M_S}}{\dot{\gamma}}, \tag{19}$$

The error analysis for M_{Sd} and T_{2d} is followed by normal distribution. The error coefficient of magnitude is 0.1, so the predicted magnitude M_{SP} could be written as

$$M_{SP} = M_{Sd} \pm 0.1 \times M_{Sd}. \tag{20}$$

The error coefficient of T_{2P} is fluctuated with M_{Sd}, so the predicted T_{2p} is

$$T_{2P} = T_{2d} \pm \alpha \cdot T_{2d}. \tag{21}$$

If $4.5 \le M_{Sd} \le 5.5$, α is 0.10. If $5.6 \le M_{Sd} \le 6.5$, α is 0.27. If $M_{Sd} \ge 6.6$, α is 0.30. The earthquake occurrence time equals the plus of T_{PP} and T_{2P}.

3. *Forecasting Attempts*

In earthquake forecasting, when the anomalous region is derived by LURR and I_t is peaked, the average seismic energy E_W and shear strain rate $\dot{\gamma}$ are determined then. The magnitude and time of a coming event in the anomalous area could be evaluated by Eqs. (18)–(21).

By the improved approach, we attempt to test some large earthquakes in recent years, prospectively. The earthquake catalog is retrieved from the China Earthquake Networks Center (CENC). Small earthquakes of $M \le 4.0$ were used to compute the LURR time series. The spatial scanning radius is 200 km, and the temporal window is 18 months with a sliding step of 1 month. The inner frictional coefficient is 0.6.

3.1. *The 2012 M_S5.3 Hami Earthquake*

The M_S5.3 event occurred in Hami, Xinjiang Autonomous Region, on Feb 10, 2012 (short for Hami M_S5.3). The epicenter is situated at 44.9°N, 93.1°E. In October 2011, we evaluated the seismic hazard for Hami, and this forecasting was published in Liu et al. 2012.

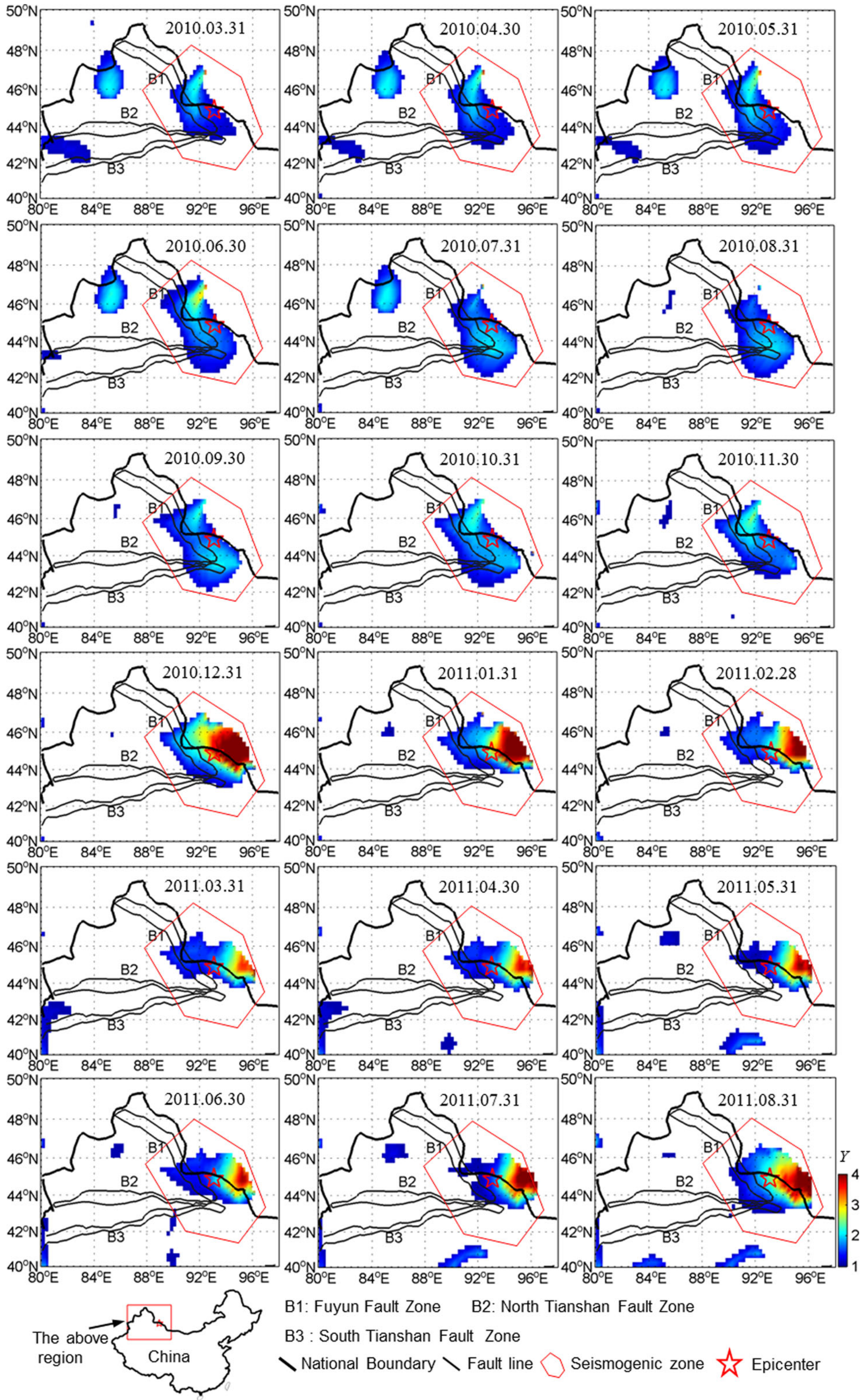

Figure 4
Sketch of the tempo-spatial evolution of LURR prior to the Hami M_S5.3

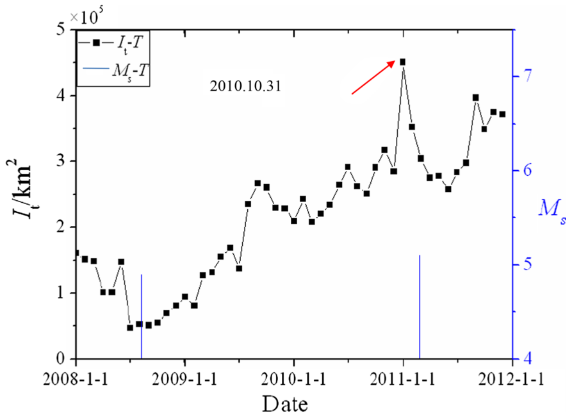

Figure 5
The temporal variation of I_t prior to the Hami M_S5.3 and earthquake sequence

The tempo-spatial evolution of LURR in the range of 40°N–50°N, 80°E–98°E during 2010-03-31 to 2011-08-31 is shown in Fig. 4. The anomalous area and the value of LURR changed from small to large, and then to small again chronologically. This change is similar to that illustrated by numerous cases studies (Wang et al. 2004; Yin et al. 2006, 2008, 2012, 2013; Yu et al. 2006; Zhang 2006). The range of the anomalous area (highlighted by red polygon in Fig. 4), $Y > 1$, and the value of LURR increased from the beginning of 2010 and started to decrease in the beginning of 2011. The temporal variation of the physical parameter I_t is shown in Fig. 5. The curve of I_t started to rise in the beginning of 2009, and reached its peak point in December 2010, with $I_{PP} = 4.52 \times 10^5 km^2$. The value of shear strain rate $\dot{\gamma}$ and average seismic energy E_W is determined when I_t is peaked. According to the GPS observations (Shen et al. 2003; Gu et al. 2001), $\dot{\gamma}$ is $(7 \sim 12) \times 10^{-9}$/a. The value of E_W is $(1.0–1.2) \times 10^9$ J/(km^2.a) (Liu et al. 2012). Then M_{SP} and T_{2P} are derived by formulas (18)–(21), for $M_{SP} = 5.5 \pm 0.5$, $T_{2P} = 17 \pm 2$ months. Here, T_{PP} is December 2010, so the earthquake may occur in March to July, 2012.

Actually, on Feb 10, 2012, the M_S5.3 event occurred in this region. The observed time is just only 1 month ahead of the prediction. The observed magnitude and the epicenter are in the range of the prediction.

3.2. *The 2013 Songyuan Earthquake Swarm*

Another example is the earthquake swarm (as shown in Table 1) that occurred in Songyuan, Jilin Province, in the end of October and November, 2013, which may be caused by the activity of Tanlu fault zone. Before the earthquake swarm, LURR anomalies were detected around the Tanlu fault zone. The prospective study was cumulated in July 2012.

Tracking studies of the LURR anomalies of Tanlu fault zone had been conducted from 2010 to 2013. The tempo-spatial distribution of LURR for the region of 28°N–46°N, 110°E–127°E from 2010-01-01 to 2013-10-31 is given in Fig. 6. There were several small anomalous regions in the beginning of 2010. Then the small anomalous regions evolve to a large one in the middle of 2011, and the degree of anomalies reached a high level. The evolutions of LURR indicated an earthquake or earthquakes would occur in or around the anomalous region. The temporal variation of parameter I_t is given in Fig. 7. I_t was going up from January to June 2011, with the peak value of $I_{PP} = 9.6 \times 10^5 km^2$, and reduced since July 2011.

In space, the anomalies cover a relatively wide range (as shown in Fig. 6). In order to optimize the

Table 1

The earthquakes with $M_S \geq 5$ occurred in Songyuan 2013

Occurrence time	latitude	longitude	deep	M
2013/10/31	44.7	124.1	10	5.7
2013/10/31	44.7	124.2	10	5.1
2013/11/22	44.7	124.1	8	5.3
2013/11/23	44.6	124.1	9	5.8
2013/11/23	44.6	124.1	8	5.0

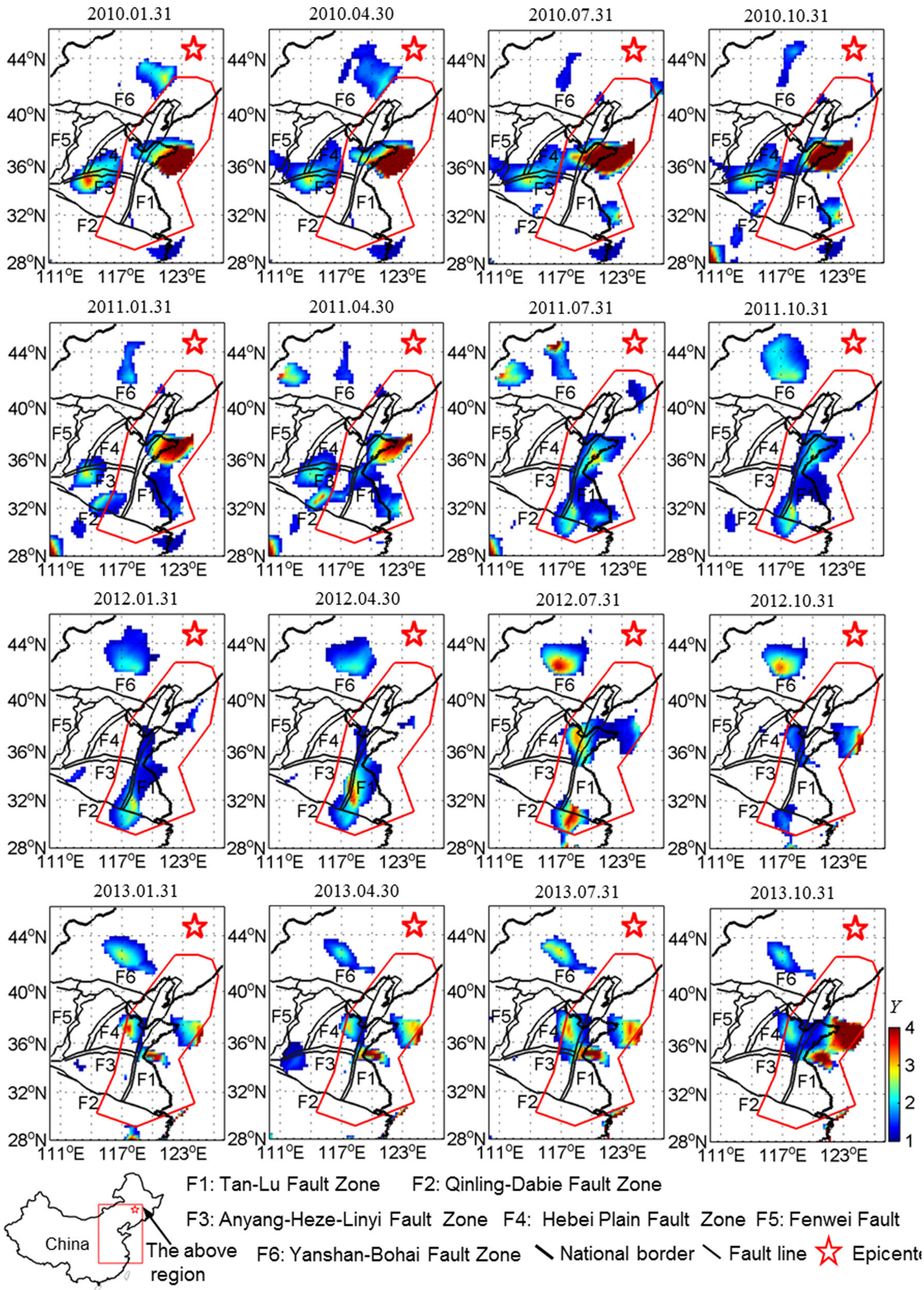

2010.01.31
2010.04.30
2010.07.31
2010.10.31
2011.01.31
2011.04.30
2011.07.31
2011.10.31
2012.01.31
2012.04.30
2012.07.31
2012.10.31
2013.01.31
2013.04.30
2013.07.31
2013.10.31
44°N
40°N
36°N
32°N
28°N
111°E
117°E
123°E
F1
F2
F3
F4
F5
F6
Y
4
3
2
1
China
The above region
F1: Tan-Lu Fault Zone
F2: Qinling-Dabie Fault Zone
F3: Anyang-Heze-Linyi Fault Zone
F4: Hebei Plain Fault Zone
F5: Fenwei Fault
F6: Yanshan-Bohai Fault Zone
National border
Fault line
Epicent

◀Figure 6
Sketch of the tempo-spatial evolution of LURR prior to the Songyuan earthquake swarm

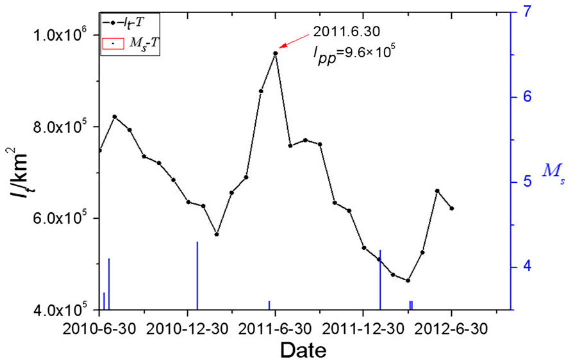

Figure 7
The temporal variation of I_t prior to the Songyuan earthquake swarm and earthquake sequence

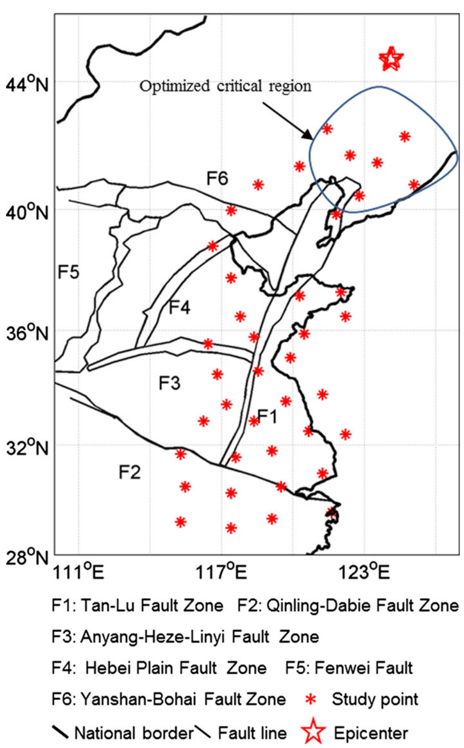

Figure 8
The optimized critical region (circled by blue curve)

seismic region, multiple sample points marked by red asterisks in Fig. 8 were analyzed. The shear strain rate is little than 1×10^{-8}/a (Shen et al. 2003; Gu et al. 2001), and the E_W is about 1.1×10^9 J/(km^2.a) (Liu et al. 2012). After estimation, the critical region is Yingkou–Haicheng–Panjin and its north (the region curved by blue line in Fig. 8) (Liu 2014), and the magnitude is 6.0 ± 0.6. The time interval T_{2P} is 24 months, so the earthquakes may occur in September 2012 to February 2014.

For about 15 months after the prospective study, an M_S5.7 earthquake occurred in Songyuan of Jilin province on October 31, 2013, and four $M_S \geq 5$ earthquakes occurred in November 2013. The epicenters are not situated in the optimized critical region, but not far from it. The seismic activity of Tanlu fault zone may make an influence on the occurrence of the Songyuan earthquake swarm. The released seismic energy and the earthquake time are in the f range of forecasting.

3.3. The 2015 M_S5.8 Alashan Earthquake

The M_S5.8 earthquake took place in Alashan league in the Inner Mongolia Autonomous Region on April 15, 2015. The epicenter is at 39.8°N and 106.3°E. Prior to the earthquake occurrence, the LURR anomalies cover part of Gansu–Ningxia–Shanxi–Inner Mongolia region. The tempo-spatial evolution of LURR for the range of 34°N–42.5°N, 100°E–112°E from 2013-09-30 to 2014-06-30 is given in Fig. 9. It is found that the anomalous area (highlighted by red polygon in Fig. 9) and the value of LURR changed from small to large, and then to small again chronologically. The temporal variation of parameter I_t (Fig. 10) shows that the value of I_t was rising from the second half of 2012 to December 2013, with $I_{PP} = 5.76 \times 10^5$km^2. So the region circled by red polygon could be seen as seismic hazard region. The shear strain rate is $(6–20) \times 10^{-9}$/a (Shen et al. 2003; Gu et al. 2001), and the value of E_W is $(2.5–3.0) \times 10^9$ J/km^2.a (Liu et al. 2012). According to the improved method, the seismic hazard region is optimized from the large red polygon to the small blue one (Fig. 11), for $M_{SP} = 6.4 \pm 0.5$ and $T_{2P} = 17$ months. So the forecasted occurrence time is from November 2014 to the end of 2015. This prediction was made on Oct 16, 2014, and relevant report was submitted to Annual Consultation.

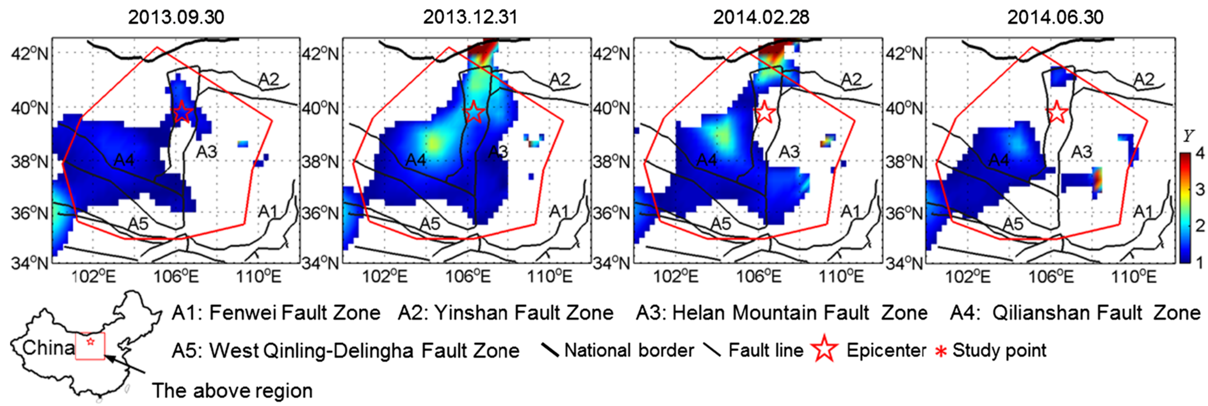

Figure 9
Sketch of the tempo-spatial evolution of LURR before the Alashan M_S5.8 earthquake

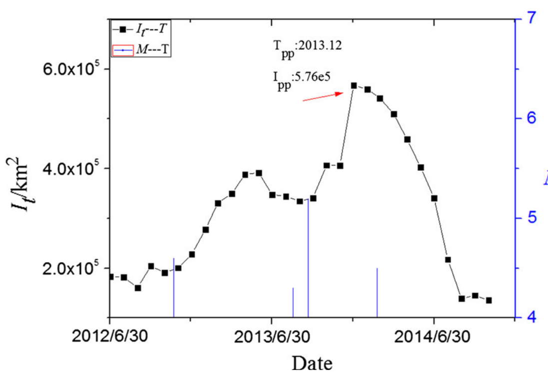

Figure 10
The temporal variation of I_t and earthquake sequence of seismogenic zone before the Alashan M_S5.8 earthquake

About 6 months after the prediction, the Alashan M_S5.8 earthquake occurred near the critical region. The forecast time is correlated well with the observed. The observed magnitude is 0.1 less than the lower limit of prediction.

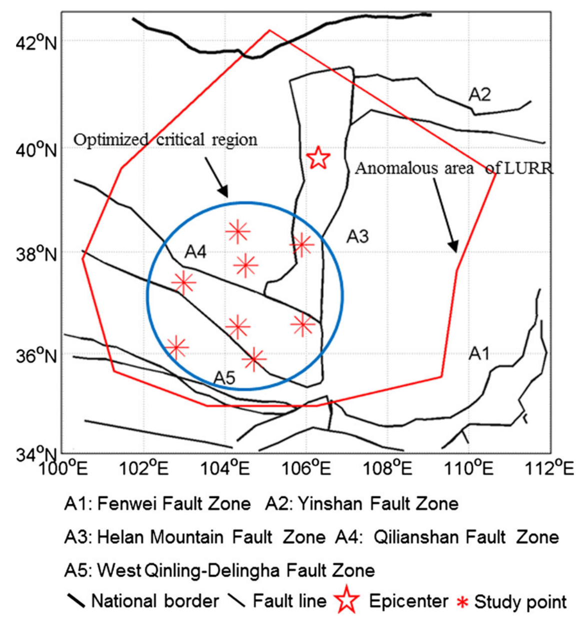

Figure 11
The optimized critical region (circled by blue curve)

3.4. The 2015 M_S8.1 Gorkha, Nepal Earthquake

Compared to the above three cases, the prediction of the 2015 M_S8.1 Gorkha, Nepal earthquake is quite different, such as in space the anomalous region is widely too large. The epicenter of Nepal M_S8.1 is situated at 28.2°N and 84.7°E, about 50 km away from Nepal–China border. A significant LURR anomaly has been covered a large area including Tibet, Yunnan, Guizhou, Sichuan, Qinghai, Guangxi, Guangdong, and the boundary region between China and Nepal, India, Burma, and Pakistan (Fig. 12) for several years. The above region is called the "pan Southwestern region" (Yin et al. 2008).

Tracking studies of LURR and seismic tendency for the above region have been conducted since 2008. According to the temporal variation of the parameter I_t of the anomalous region, we could find that I_t reached its peak value in July 2012 (Fig. 13). According to the synthesis approach, we predict that a strong earthquake of $M_S = 8.6 \pm 0.7$ may occur in the "pan

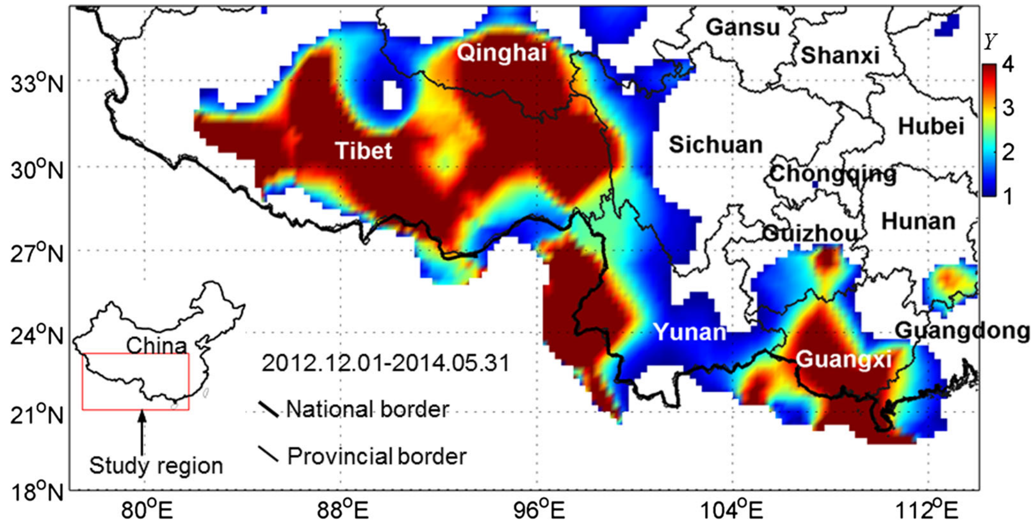

Figure 12
Distribution of LURR anomalies prior to the 2015 M_S8.1 Gorkha, Nepal Earthquake

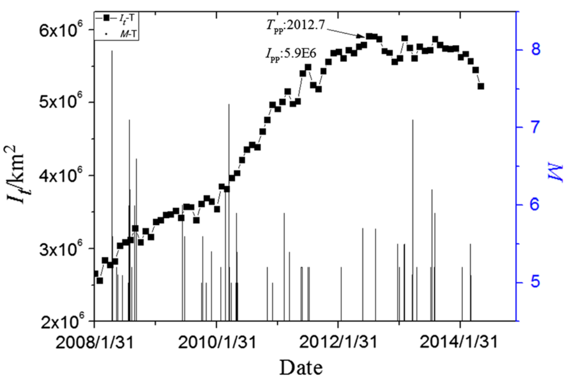

Figure 13
The temporal variation of I_t for the "pan Southwestern region"

Southwestern region" during July 2015 ± 25 months (Liu 2014; Yin and Liu 2014), which was last issued at SCA 2014 (Conference on Supercomputing Applications of Chinese Academy Sciences in 2014) on August 21-25, 2014. Indeed the 2015 M_S8.1 Gorkha, Nepal earthquake occurred in the range of forecast. Although in space related to the forecast covers a very wide range, the result is also inspiring.

4. Discussion and Conclusion

The dimension analysis technique presented in this paper is devised to better optimize the earthquake critical region, magnitude, and time after the tempo-spatial scanning of LURR having been conducted and anomalous area having been detected. To investigate the effect of the areal variation on LURR anomalies, the geophysical quantities of average seismicity (E_W) and shear strain rate ($\dot{\gamma}$) are taken into consideration. A significant connection exists in the heterogeneity of the crust media, the shear strain rate, and seismicity. If the LURR anomalous area is wide in space, E_W and $\dot{\gamma}$ for some region may great lager than the others. According to the improved results from (Eqs. (18)–(21)), big difference may exist in the assessed magnitude and time for different study points. Then we could screen out the points with less occurrence potential of earthquake, such as very low magnitude, and retain the points with reasonable occurrence magnitude and time; hence the critical region is optimized and the occurrence of false alarms is effectively reduced. Our dimensional analysis technique may help us quantitatively assess the occurrence time and magnitude of future earthquakes as well as the critical regions of the anomalous area given by LURR.

It should be pointed out that the selection of the physical quantities plays a key role for dimensional analysis. Due to the limitation of observation technique, some important parameters, such as rock strength, elastic modulus, and fracture toughness are not used here, and average seismic energy and shear strain rate are analyzed. The data quantity also counts a great deal. More earthquake cases should be investigated in different area and different periods. Due to the limitation, just only 50 earthquakes that occurred in Chinese mainland since 1976 were analyzed.

Generally speaking, there is more work to do to augment the predictive power of LURR. In optimizing the seismic hazard region, LURR could combined with other method, such as PI (Rundle et al. 2002; Yu et al. 2013, 2016; Zhang et al. 2016), which has shown considerable promise.

Acknowledgements

The catalog data are taken from the China Earthquake Networks Center (CENC). The shear strain data are provided by Professor Zai-sen Jiang, Zheng-kang Shen and Guo-hua Gu. Parts of the calculations in the paper are conducted in Supercomputing Center of Computer Network information Center, Chinese Academy of Sciences (CAS). Professor Huai-zhong Yu gives constructive advices. This research is supported by the Institute of Earthquake Forecasting CAE (2015IES0102). We are grateful here.

References

Aki, K. (1965). Maximum likelihood estimate of b in the formula logN = a-bm and its confidence limits. *Bulletin of the Earthquake Research Institute, Tokoyo university, 43,* 237–239.

Bai, Y. L., Xia, M. F., Ke, F. J., & Li, H. L. (2002). Closed trans-scale statistical microdamage mechanics. *Acta Mechanica Sinica, 18,* 1–17.

Bowman, D. D., Ouillen, G., Sammis, C. G., Sornette, A., & Sornette, D. (1998). An observational test of the critical earthquake concept. *Journal of Geophysical Research, 103,* 24359–24372.

Buckingham, E. (1914). On physically similar systems: Illustrations of the use of dimensional analysis. *Physical Review, 4,* 345–376.

Gu, G. H., Shen, X. H., Wang, M., Zheng, G. M., Fang, Y., & lI, P. (2001). General characteristics of the recent horizontalcrustal movement in Chinesemainland. *Acta Seismological Sinica, 23,* 362–369.

Gutenberg, B., & Richter, C. F. (1944). Frequency of earthquakes in California. *Bulletin of the Seismological Society of America, 34,* 185–188.

Jaume, S. C., & Sykes, L. R. (1999). Evolving towards a critical point: a review of accelerating seismic moment/energy release prior to large and great earthquakes. *Pure and Applied Geophysics, 155,* 279–306.

Jiang, Z. S., Ma, Z. J., Zhang, X., Wang, Q., & Wang, S. X. (2003). Horizontal strain field and tectonic deformation of china mainland revealed by preliminary GPS result. *Chinses J Geophysics, 46,* 352–358.

Kachanov, L. M. (1986). *Introduction to continuum damage mechanics*. Dordrecht: MartinusNijhoff Publishers.

Kasahara, K. (1981). *Earthquake mechanics*. Cambridgo: Cambridge University Press.

Lemaitre, J. (1992). *A course on damage mechanics*. Berlin/Heidelberg: Springer-Verlag.

Li, H. L., Bai, Y. L., Xia, M. F., Ke, F. J., & Yin, X. C. (2000). Damage localization as a possible precursor of earthquake rupture. *Pure and Applied Geophysics, 157,* 1929–1943.

Li, Y. X., Li, Z., & Zhang, J. H. (2004). Horizontal strain field in the Chinese mainland and its surrounding areas. *Chinese Journal of Geophysics, 47,* 222–231. **(in Chinese with English abstract)**.

Liu Y (2014) Study of several issues concerning Load-Unload Response Ratio in Earthquake Prediction. PhD Thesis of the Graduate School of the Chinese, Academy of Sciences (**in Chinese with English abstract**).

Liu, Y., Yin, X. C., Yuan, S., & Zhang, L. P. (2012). Exploration study of dimensional analysis applying to earthquake prediction. *Chinese Journal of Geophysics, 55,* 3043–3050. **(in Chinese with English abstract)**.

Melchior, P. (1983). *The tides of the planet Earth*. Oxford: Pergamon Press.

Reches, Z., & Lockner, D. A. (1994). Nucleation and growth of faults in brittle rocks. *Journal of Geophysical Research, 99,* 18159–18173.

Rundle, J. B., Tiampo, K. F., Klein, W., & Martins, J. S. S. (2002). Self-organization in leaky threshold systems: The influence of near-mean field dynamics and its implications for earthquakes, neurobiology, and forecasting. *Proceedings of the National academy of Sciences of the United States of America, 99,* 2514–2521.

Scholz, C. H., Sykes, L. R., & Aggrawal, Y. P. (1972). Earthquake prediction: A physical basis. *Science, 181,* 803–810.

Sedov, L. I. (1959). *Similarity and dimensional methods in mechanics[M]*. London: Academic Press.

Shen, Z. K., Wang, M., Gan, W. J., & Zhang, Z. S. (2003). Contemporary tectonic strain rate field of chinese continent and its geodynamic implications. *Earth Science Frontiers, 10*(suppl), 93–100.

Song, Z. P., Yin, X. C., Wang, Y. C., Xu, P., & Xue, Y. (2000). The tempo-spatial evolution characteristics of the load/unload response ratio befor strong earthquakes in California of America and its predicting implication. *Acta Seismological Sinica, 22*(6), 588–595. **(in Chinese with English abstract)**.

Tan, Q. M. (2011). *Dimensional analysis: with case studies in mechanics[M]*. New York: Springer Science & Business Media.

Wang, Y. C., Yin, C., Mora, P., Yin, X. C., & Peng, K. Y. (2004). Spatio -temporal scanning and statistical test of the accelerating moment release (AMR) model using Australian earthquake data. *Pure and Applied Geophysics, 161,* 2281–2293.

Yang, S. M., Li, J., & Wang, Q. (2008). The deformation pattern and fault rate in the Tianshan Mountains inferred from GPS observations. *Science in China, Series D: Earth Sciences, 51*(8), 1064–1080.

Yin, X. C. (1987). A new approach to earthquake prediction. *Earthquake Research in China, 3,* 1–7. **(in Chinese with English abstract)**.

Yin, X. C. (1993). A new approach to earthquake prediction. *Russia's "Nature", 1,* 21–27. **(in Russian)**.

Yin, X. C., Chen, X. Z., Song, Z. P., & Yin, C. (1995). A new approach to earthquake prediction: the load/unload response ratio (lurr) theory. *Pure and Applied Geophysics, 145,* 701–715.

Yin, X. C., & Liu, Y. (2014). Load-Unload response ratio-an interplay between earthquake prediction and mechanics. *Advances in Mechanics, 43,* 555–580. **(in Chinese with English abstract)**.

Yin, X. C., Liu, Y., Peter, M., Yuan, S., & Zhang, L. P. (2013). New progress in LURR-integrating with the dimensional method. *Pure and Applied Geophysics, 170,* 229–236.

Yin, X. C., Liu, Y., & Zhang, L. P. (2012). Load-unload response ratio and its new progress[M]. In Y. G. Li (Ed.), *Imaging, modeling and assimilation in seismology* (pp. 219–244). Boston: High Education Press and Walter De Gruyter GmbH & Co. KG.

Yin, X. C., Mora, P., Peng, K. Y., Wang, Y. C., & Weatherly, D. (2002). Load-unload Response Ratio and Accelerating Moment/Energy Release, Critical Region Scaling and Earthquake Prediction. *Pure and Applied Geophysics, 159,* 2511–2524.

Yin, X. C., Zhang, L. P., Zhang, H. H., Yin, C., Wang, Y. C., Zhang, Y. X., et al. (2006). LURR's twenty years and its perspective. *Pure and Applied Geophysics, 163,* 2317–2341.

Yin, X. C., Zhang, L. P., & Zhang, Y. X. (2008). LURR anomoly with great tempo-spatial scale before large earthquake-Prediction of the upcoming great earthquake in the Chinese mainland. *The researches on prediction of the strong earthquake tendency for Chinese mainland in 2009* (pp. 144–150). Beijing: Seismological Press.

Yu, H. Z., Cheng, J., & Wan, Y. G. (2015). The sensitivity of loa/unload response ratio and critical region selection before large earthquakes. *Pure and Applied Geophysics, 172,* 2203–2214.

Yu, H. Z., Cheng, J., Zhang, X. T., Zhang, L. P., Liu, J., & Zhang, Y. X. (2013). Multi-methods combined analysis of the future earthquake potential. *Pure and Applied Geophysics, 170,* 173–183.

Yu, H. Z., Cheng, J., Zhu, Q. Y., & Wan, Y. G. (2011). Critical sensitivity of load/unload response ratio and stress accumulation before large earthquakes: Example of the 2008 M_W7.9 Wenchuan Earthquake. *Natural Hazards, 58*(1), 251–267.

Yu, H. Z., Shen, Z. K., Wan, Y. G., & Zhu, Q. Y. (2006). Increasing critical sensitivity of the Load/Unload Response Ratio before large earthquakes with identified stress accumulation pattern. *Tectonophysics, 428,* 87–94.

Yu, H. Z., Zhou, F. R., Cheng, J., Zhang, X. T., & Zhang, Y. X. (2016). Development of a combination approach for seismic hazard evaluation. *Pure and Applied Geophysics, 173,* 221–233.

Yu, H. Z., & Zhu, Q. Y. (2010). A probabilistic approach for earthquake potential evaluation based on the Load/Unload Response Ratio method. *Concurr Comp-Pract E, 22,* 1520–1533.

Zhang, H. H. (2006). Prediction of catastrophic failure in heterogeneous brittle media-study and practice of Load/Unload Response Ratio (LURR). PhD Thesis of The Graduate School of the Chinese Academy of Sciences (**in Chinese with English abstract**).

Zhang, S. F., Wu, Z. L., & Jiang, C. S. (2016). The central china north–south seismic belt: seismicity, ergodicity, and five-year pi forecast in testing. *Pure and Applied Geophysics, 173,* 245–254.

Zhang, L. P., Yu, H. Z., & Yin, X. C. (2013). Failure potential evaluation in engineering experiments using Load/Unload Response Ratio Method. *Pure and Applied Geophysics, 170,* 237–245.

Zhang, L. P., & Zhuang, J. C. (2011). An improved version of the load/unload response ratio method for forecasting strong aftershocks. *Tectonophysics, 509,* 191–197.

Zohuri, B. (2015). *Dimensional analysis and self-similarity methods for engineers and scientists[M].* New York: Springer.

Zubovich, A. V., Wang, X. Q., Scherba, Y. G., et al. (2010). GPS velocity field for the Tien Shan and surrounding regions. *Tectonics*. https://doi.org/10.1029/2010TC002772.

(Received January 29, 2016, revised October 26, 2017, accepted October 28, 2017, Published online November 11, 2017)